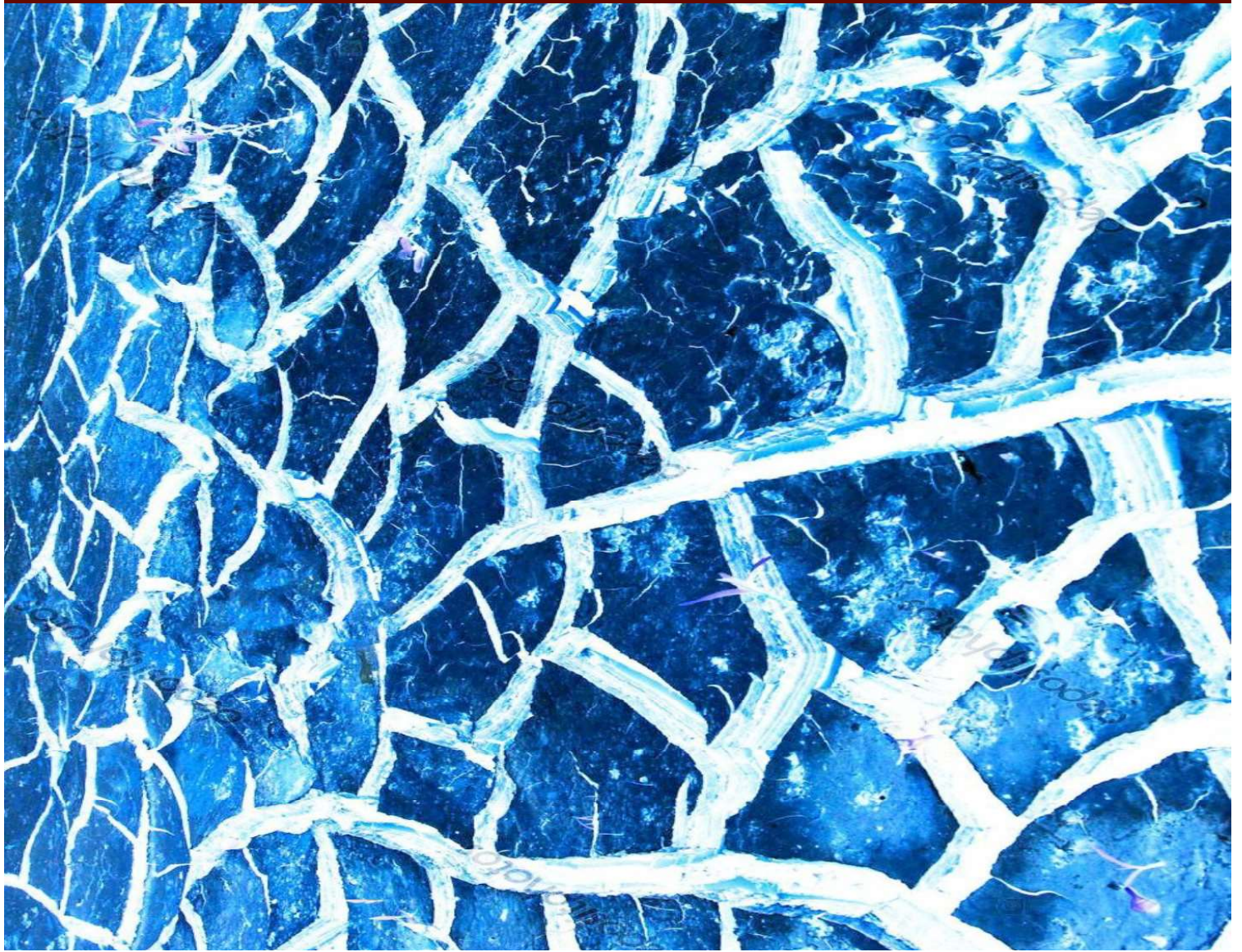


Applicable Solutions in Non-Linear Dynamical Systems



EDITORS

Jan Awrejcewicz
Marek Kaźmierczak
Paweł Olejnik

DSTA 2019

Applicable Solutions in Non-Linear Dynamical Systems

Editors

JAN AWREJCEWICZ, MAREK KAŹMIERCZAK, PAWEŁ OLEJNIK

© Copyright by Politechnika Łódzka 2019

ISBN 978-83-66287-30-3

Cover design: Marek Kaźmierczak
Technical editor: Marek Kaźmierczak

Wydawnictwo Politechniki Łódzkiej
ul. Wólczańska 223, 90-924 Łódź
tel. 42 631 20 87, fax. 42 631 25 38
e-mail: wydawnictwo@lib.p.lodz.pl

Printed by:
ARSA Druk i Reklama
90-270 Łódź, ul. Piotrkowska 4
tel./fax (042) 633 02 52
marta@arsa.net.pl
www.arsa.net.pl

PREFACE

The 15th International Conference “Dynamical Systems - Theory and Applications” (DSTA 2019, 2-5 December, 2019, Lodz, Poland) gathered a numerous group of outstanding scientists and engineers who deal with widely understood problems of theoretical and applied dynamics.

Organization of the conference would not have been possible without great effort of the staff of the Department of Automation, Biomechanics and Mechatronics of the Lodz University of Technology. The patronage over the conference has been taken by the Committee of Mechanics of the Polish Academy of Sciences and Ministry of Science and Higher Education of Poland.

It is a great pleasure that our event was attended by over **180** researchers from **35** countries all over the world, who decided to share the results of their research and experience in different fields related to dynamical systems.

This year, the DSTA Conference Proceedings were split into two volumes entitled “*Theoretical Approaches in Non-Linear Dynamical Systems*” and “*Applicable Solutions in Non-Linear Dynamical Systems*”. In addition, DSTA 2019 resulted in three volumes of Springer Proceedings in Mathematics and Statistics entitled “*Control and Stability of Dynamical Systems*”, “*Mathematical and Numerical Approaches in Dynamical Systems*” and “*Dynamical Systems in Mechatronics and Life Sciences*”. Also, many outstanding papers will be recommended to special issues of renowned scientific journals.

The DSTA Conference Proceedings include papers covering the following topics:

- asymptotic methods in non-linear dynamics,
- bifurcation and chaos in dynamical systems,
- control in dynamical systems,
- dynamics in life sciences and bioengineering,
- engineering systems and differential equations,
- non-smooth systems
- mathematical approaches to dynamical systems
- original numerical methods of vibration analysis,
- stability of dynamical systems,
- vibrations of lumped and continuous systems,
- other problems.

Proceedings of the 15th Conference „Dynamical Systems - Theory and Applications” summarize **106** papers of university teachers and students, researchers and engineers from all over the world. The papers were selected by the Scientific Committee of DSTA 2019 from **360** papers submitted to the conference. Therefore, the reader is provided with an overview of recent developments in dynamical systems and can study the most progressive tendencies in this field of science.

Our experience shows that a broad thematic scope comprising dynamical systems encourages researchers to exchange their opinions on different branches of dynamics. We think that the vivid discussion will influence positively creativity and will result in effective solutions of many problems of dynamical systems in mechanics and physics, both in terms of theory and applications.

We do hope that DSTA 2019 will contribute to establishing new and tightening the already existing relations and scientific and technological cooperation between Polish and foreign institutions.

On behalf of both
Scientific and Organizing Committees

A handwritten signature in black ink, appearing to read 'Awrejcewicz', written in a cursive style.

Chairman
Professor Jan Awrejcewicz

CONTENTS

Nurtay Albanbay, Bekbolat Medetov, Michael Zaks <i>Distribution of lifetimes for transient bursting states in coupled noisy excitable systems</i>	11
Tariq Alzarooni, Mohammad AL-Shudeifat, Oleg Shirayev, C. Nataraj <i>On backward whirl excitation in linear time-variant intact and cracked rotor systems</i>	25
Jan Awrejcewicz, Dmytro Bilichenko, Akram Khalil Cheib, Nataliya Losyeva, Volodymyr Puzyrov <i>Estimation of the domain of attraction for a nonlinear mechanical system</i>	37
Jan Awrejcewicz, Olga Saltykova, Vadim Krysko, Anton Krysko <i>Nonlinear dynamics of flexible nanobeams taking into account the Casimir, van der Waals and Coulomb forces</i>	47
Jan Awrejcewicz, Roman Starosta, Grażyna Sypniewska-Kamińska <i>Vibration of nonlinear lumped systems with serially connected elastic elements</i>	55
Jan Awrejcewicz, Maxim Zhigalov, Sergey Pavlov, Vadim Krysko <i>Nonlinear dynamics of thermoelastic Sheremetiev-Pelekh nanobeams with topologically optimal microstructure</i>	65
Włodzimierz Bielski, Ryszard Wojnar <i>Gravity waves in channels with corrugated bottom: asymptotic approaches</i>	75
Ivan Bizyaev, Alexey Borisov, Alexander Kilin, Ivan Mamaev, Elena Pivovarova <i>Nonholonomic acceleration and chaotic dynamics of locomotion</i>	87
Vasily Buyadzhi, Anna Buyadzhi, Alexey Chernyshev, Evgeniya Plisetskaya, Eugeny Pavlov, Sergey Kir'yanov <i>Nonlinear dynamics of laser systems: Chaos, bifurcations and strange attractors</i>	99
Jarosław Chruściel, Anna Frątczak, Angelika Puchalska, Siam Streibl, Bartłomiej Zagrodny <i>Thermographic analysis of the additional load influence on the muscle activation during gait</i>	107
Stefan Chwastek <i>Finding globally optimal combinations of cranes drive mechanisms by the method of exhausting alternative design structures of mechanisms</i>	117

Eva-H. Dulf , Cristina-I. Muresan , Daniel D. Timis	
<i>Adaptive fractional order control of a quadrotor</i>	129
Wiesław Fiebig	
<i>The use of mechanical resonance for the reduction of torque pulsation and energy demand in machines with crankshaft systems</i>	139
Gustavo de Freitas Fonseca , Airton Nabarrete	
<i>Finite element analysis of magneto-rheological fluid embedded on journal bearings</i>	151
Mirosław Gidlewski , Leszek Jemioł , Dariusz Żardecki	
<i>Influence of control system parameters and it's disturbances on lane change process</i>	163
Aurélien Grolet , Zein Shami , Sadaf Arabi , Olivier Thomas	
<i>Experimental nonlinear localisation in a system of two coupled beams</i>	171
Dariusz Grzelczyk , Jan Awrejcewicz	
<i>Stability and control of a hybrid walking robot on planar, unstable and vibrating terrain</i>	183
Ben Gunn , Stephanos Theodossiades , Steve Rothberg	
<i>A rotational energy harvester for propulsion systems: design and experimental validation</i>	193
Nicolae Herisanu , Vasile Marinca	
<i>A new analytical approach to nonlinear free vibration of microtubes</i>	205
Elżbieta Jarzębowska , Krzysztof Augustynek , Andrzej Urbaś	
<i>Dynamics and vibration analysis of a spatial linkage model with flexible links and joint friction subjected to position and velocity motion constraints</i>	215
Olga Jarzyna , Dariusz Grzelczyk , Jan Awrejcewicz	
<i>A simple pattern generator for biped walking</i>	227
Kalkunte R. Jayaprakash , Yuli Starosvetsky	
<i>Analytical and numerical study of piecewise linear Mathieu equation with non-zero offset</i>	237
Krzysztof Kaliński , Marek Galewski , Michał Mazur , Natalia Morawska	
<i>Optimization of the spindle speed during milling of large-sized structures with the use of technique of Experiment-Aided Virtual Prototyping</i>	249

Olga Yu. Khetselius , Andrey A. Svinarenko , Yuliya Ya. Bunyakova , Alexander V. Glushkov	
<i>Chaos-geometric approach to analysis and forecasting evolutionary dynamics of complex systems: Atmospheric pollutants dynamics</i>	259
Olga Yu. Khetselius , Andrey A. Svinarenko , Anna V. Ignatenko , Anna A. Buyadzhi	
<i>New generalized chaos-geometric and neural networks approach to nonlinear modeling of complex chaotic dynamical systems</i>	267
Anton Krysko , Jan Awrejcewicz , Ilya Kutepov , Vadim Krysko	
<i>Nonlinear dynamics of NEMS resonators in temperature field</i>	277
Vadim A. Krysko-jr , Jan Awrejcewicz , Maxim V. Zhigalov , Vadim. A. Krysko	
<i>Dimension reduction method in nonlinear equations of mathematical physics (MEMS/NEMS problems)</i>	289
Vadim A. Krysko-jr , Jan Awrejcewicz , Ekaterina Yu. Krylova , Irina V. Papkova	
<i>Nonlinear dynamics of flexible nanoplates resting on an elastic foundation in a stationary temperature field</i>	301
Izabela Krzysztofik , Zbigniew Koruba	
<i>An optimal control of the gyroscope system in the process of homing an air-to-air missile</i>	313
Paweł Latosiński , Andrzej Bartoszewicz	
<i>Discrete-time model reference sliding mode control using an exponential reaching law</i>	323
Enrique Roberto Carrillo Li , Philipp Schorr , Tobias Kaufhold , Jorge Antonio Rodríguez Hernández , Lena Zentner , Klaus Zimmermann , Valter Böhm	
<i>Kinematic analysis of the rolling locomotion of mobile robots based on tensegrity structures with spatially curved compressed components</i>	335
António M. Lopes , J.A. Tenreiro Machado	
<i>Fractional dynamics and power law behavior in soccer leagues</i>	345
Alexey Lukin , Popov Ivan , Udalov Pavel	
<i>Nonlinear dynamics of the sensory element of the atomic force microcopy</i>	355
Olga Mazur , Jan Awrejcewicz	
<i>Size-dependent nonlinear vibrations of micro-plates subjected to in-plane magnetic field</i>	365
Ewelina Ogińska , Krystian Polczyński , Dariusz Grzelczyk , Jan Awrejcewicz	
<i>Numerical and experimental investigations of dynamics of magnetic pendulum with an aerostatic bearing</i>	375

Alexey Papirovskiy , Alexey Lukin , Ivan Popov <i>Analytical and numerical modelling of surface acoustic waves in rotating media</i>	387
Wojciech Paszowski , Tomasz Bartkowiak <i>Dynamics of logistic train</i>	397
Leon Prochowski , Mateusz Ziubiński , Patryk Szwajkowski , Tomasz Pusty , Mirosław Gidlewski <i>Experimental and simulation examination of the impact of the control model on the motion of a motorcar with a trailer in a critical situation</i>	409
Andrzej Rysak , Magdalena Gregorczyk <i>Study of the Duffing van der Pol system dynamics using RQA measures</i>	423
Alireza Ture Savadkoohi , Claude-Henri Lamarque , Célien Goossaert <i>Control of tremors of human's arm by a passive nonlinear absorber</i>	431
Yury Selyutskiy <i>Alternation of stability character in systems with positional non-conservative forces</i>	439
Aleksander Skurjat <i>The influence of lateral swaying on the trajectory of articulated rigid body vehicles</i>	449
Valeri Smirnov , Leonid Manevitch <i>Strong mode coupling in vibrations of single-walled carbon nanotubes</i>	457
Anna Šmeringaiová , Imrich Vojtko <i>Experimental assessment of the test station support structure rigidity by the vibration diagnostics method</i>	469
Rafael Teloli , Samuel da Silva , Gaël Chevallier <i>Parameters estimation by harmonic probing of hysteresis models of bolted jointed</i>	479
Valentin Ternovsky , Alexander Glushkov , Eugeny Ternovsky , Andrey Tsudik <i>Dynamics of non-linear processes in a backward-wave tubes chain: Chaos and strange attractors</i>	491
Hans True <i>Bifurcations and transitions in railway vehicle dynamics</i>	499
Ferdinand Verhulst <i>Systems with fast limit cycles and slow interaction</i>	511

Wiktorija Wojnicz , Bartłomiej Zagrodny , Michał Ludwicki , Jerzy Mrozowski , Jan Awrejcewicz , Edmund Wittbrodt <i>Multibody models for gait analysis</i>	523
Kiyotaka Yamashita , Naoto Nishiyama , Kohsuke Katsura , Hiroshi Yabuno <i>Nonlinear stability of a spring-supported pipe conveying fluid</i>	539
Azhar Ali Zafar , Jan Awrejcewicz <i>On the dynamics of blood through the circular tube along with magnetic properties</i>	547
Klaus Zimmermann , Igor Zeidis , Victor Lysenko , Simon Gast , Lars Günther , Florian Schale , Michel Rohn <i>Mathematical model and a prototype of a linear motor controlled by a periodic magnetic field</i>	559
Ádám Zsiros , János Lelkes , Tamás Kalmár-Nagy <i>Energy spectrum of inhomogeneous rods with elastic and viscous boundary conditions</i>	567

Multibody models for gait analysis

Wiktoria Wojnicz, Bartłomiej Zagrodny, Michał Ludwicki,
Jerzy Mrozowski, Jan Awrejcewicz, Edmund Wittbrodt

Abstract: The aim of this study was to create multibody biomechanical models to analyze a normal gait of the human. Proposed models can be used to identify joint moments of the lower limbs during normal gait in the single and double support phases. Applying Newton-Euler formulation, following planar models were developed: 1) a mathematical 6DOF model describing a gait in the sagittal plane of the body for single support phase and double support phase; 2) a mathematical 7DOF model describing a gait in the sagittal plane of the body for single support phase and double support phase; 3) a mathematical 7DOF model describing a gait in the frontal plane of the body for single support phase and double support phase. Proposed mathematical models can be applied to solve a forward dynamic task or inverse dynamic task. A validation of these models had been performed by comparing results measured over examination of normal human gait and results calculated by solving an inverse dynamic task.

1. Introduction

From the mechanical point of view a gait of the human is considered as periodical movements of lower limbs that alternately generate stable and unstable states. Over each phase of the gait a body weight is propelled by maintaining a stable posture due to functioning of posture-stabilizing mechanisms controlled by the human nervous system. A normal gait occurs when the right and left parts of the human body perform similar motions with respect to the anatomical planes of the body. This gait can be analyzed by deriving planar dynamic models describing motions occurring in a sagittal and frontal plane of the body. A pathological gait occurs when the right and left parts of the human body perform asymmetrical motions in space. To analyze this gait the spatial dynamic models should be derived.

A human body is treated as a musculoskeletal system composed of segments having defined number of degrees of freedom (DOFs). Net joint moments, net joint intersegmental forces and net joint powers generated in this system during gait can be estimated by using an inverse dynamics approach [11]. To solve an inverse dynamic task, the following data should be assessed: 1) biomechanical data of the subject (segment masses and dimensions; segment radii of gyration; segment moments of inertia); 2) kinematic data of human segments (joint centers, proximal and distal points of segments that are used to calculate angular displacement, angular velocity and angular acceleration of body parts); 3) kinetic data (reaction forces of interaction with the ground that can be measured by using a force plate); 4) EMG data (to estimate activity of muscles producing motion and muscle excitation timing).

A gait is composed of single and double support phases. During each double support phase a system becomes a closed system. This demands to solve an indeterminacy problem referring to estimation of external force/moment distribution.

The aim of this study was to create multibody biomechanical models to analyze a normal gait of the human and to identify joint moments of the lower limbs during all gait phases. The scope of the study was to derive dynamic models to analyze: 1) single support phase (open sagittal 6DOF model, open sagittal 7DOF model and open frontal 7DOF model); 2) double support phase, which occurs due to interaction between the sole of the swinging leg and a ground (closed sagittal 6DOF model, closed sagittal 7DOF model and closed frontal 7DOF model)..

2. Materials and Methods

A human body was treated as a multibody system composed of two ankle joints, two knee joints and one hip joint (sagittal models) or two hip joints (frontal models). An influence of the upper part of the body (the pelvis, torso, head, neck and upper limbs) was modelled by using two approaches. The first one implies that the upper part of the body is modelled as one concentrated force applied at the center of gravity of the upper body part. An influence of this force is modelled as a load (force and its moment) transmitted through the hip joint to the stance leg (single support phase) or both legs (double support phase). This approach was adapted to create a sagittal 6DOF model and a frontal 7DOF model. The second approach treats the upper part of the body as one additional segment, which is connected to the hip joint. This approach was adapted to create a sagittal 7DOF model.

To simulate behavior over single and double support phases (Fig.1) there were proposed two different type of models: open sagittal 6DOF model and closed sagittal 6DOF model; open sagittal 7DOF model and closed sagittal 7DOF model; open frontal 7DOF model and closed frontal 7DOF model. It should be mentioned that the Fig.1 illustrates behavior of the 6DOF model (behavior of each 7DOF model is similar).

Biomechanical multibody models presented in this paper were derived by applying Newton-Euler formulation [1,4]. Proposed biomechanical model can be applied to analyze forward or inverse dynamics problems. It is worth noticing that proposed models are more complex ones with respect to the models presented in [5-6, 12].

It should be mentioned that real biomechanical system is composed of joints that are linking neighboring segments through passive tissues (bursa, ligaments, tendons) and active tissues (muscles). An influence of both tissues can be considered by inputting rheological models composed of viscoelastic elements. These elements are also implemented in the joints of proposed biomechanical models.



An approach to solve a problem with interaction, which occurs when the heel of the swing leg strikes the ground (initiation of the double support phase), is described in the below subsection referring to the interaction modelling. Considering a homogeneous mass distribution, the segmentation (i.e. body partitioning) was performed according to Zatsiorsky's method [2-3]. Proposed biomechanical models were implemented in MATLAB software by creating author programs.

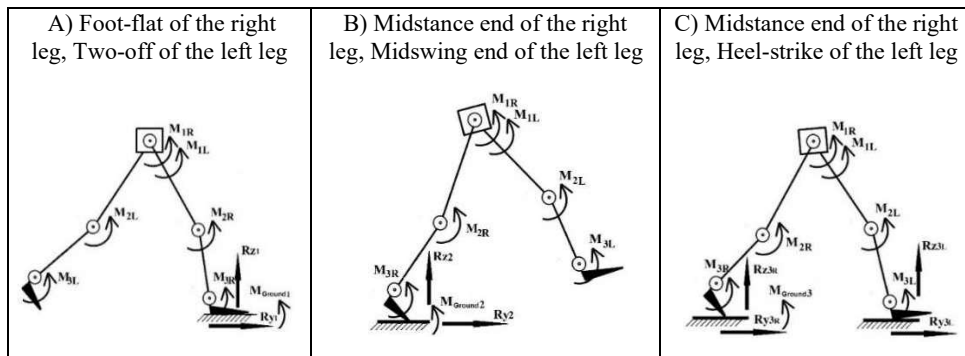


Figure 1. Structural 6DOF model in the single support phase (A, B) and double support phase (C): $M_{Ground1}$ – the ground moment during the single support phase (A), $M_{Ground2}$ – the ground moment during the single support phase (B), $M_{Ground3}$ – the ground moment during the double support phase (C); R_{yj} – the y -th component of the leg reaction force (anterior-posterior component) during the j -th single support phase ($j = 1,2$); R_{zj} – the z -th component of the leg reaction force (vertical component) during the j -th single support phase ($j = 1,2$); R_{z3R} and R_{z3L} – the z -th components of the reaction force of the right and left leg during the double support phase; R_{y3R} and R_{y3L} – the y -th components of the reaction force of the right and left leg during the double support phase; M_{iL} – i -th moment acts at the i -th joint of the left leg; M_{iR} – i -th moment acts at the i -th joint of the right leg

Sagittal 6DOF model

Considering the body as a structure composed of six segments serially linked through the hinge joints in a sagittal plane, there were created two models (Fig. 2): 1) open sagittal 6DOF model, which can be applied to model a single support phase (in this case both y -th (F_y) and z -th (F_z) components of reaction force of the swing leg are equal to zero); 2) closed sagittal 6DOF model, which can be used to describe a double support phase. Both models can be applied to analyze kinematics and dynamics of normal gait in a sagittal plane over specific phases. An influence of the upper part of the body was modelled as one concentrate force G_7 (it is a gravity force of upper part of the body) and the moment of this force M_{G7} . It was assumed that this force and its moment influence the stance leg. The hinge joint O models the metatarsophalangeal joint of the stance feet by assuming that it does not cause any dissipation phenomenon. A complete mathematical models of the open sagittal 6DOF model and closed sagittal 6DOF model are described in [8-9].

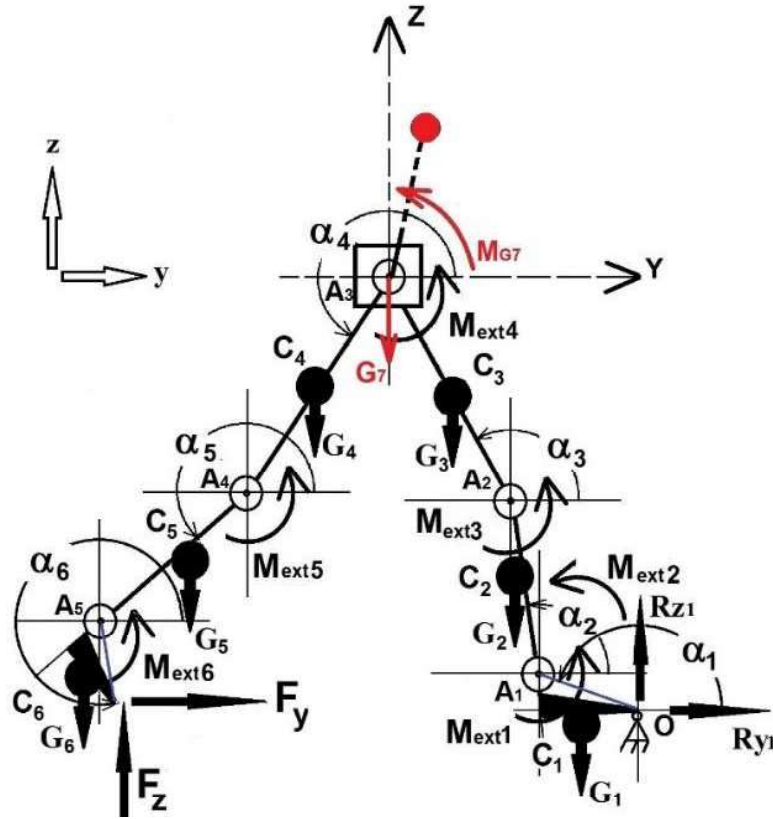


Figure 2. The sagittal 6DOF model (O – the point between the support foot and the ground (the metatarsophalangeal joint); A_1 – the ankle joint of stance leg; A_2 – the knee joint of stance leg; A_3 – the hip joint; A_4 – the knee joint of swing leg; A_5 – the ankle joint of swing leg; α_i – the angle of the i -th segment (each angle is measured as an absolute coordinate); G_i – the gravity force of the i -th segment that acts at its center of gravity C_i ; M_{ij} – the net joint moment between the i -th segment and j -th segment ($M_{ij} = M_{ji}$); M_{exti} – the external moment loading the i -th segment; R_{y1} – the y -th component of stance leg reaction force (anterior-posterior component); R_{z1} – the z -th component of the stance leg reaction force (vertical component); F_y and F_z – the y -th and z -th component of reaction force of the swing leg during double supporting phase; y – the sagittal axis; z – the vertical axis) [9]

Sagittal 7DOF model

Considering the body as a dendritic structure composed of seven segments in a sagittal plane, there were created (Fig. 3): 1) the open sagittal 7DOF model, which can be applied to model a single support phase (in this case both the y -th (F_y) and z -th (F_z) components of reaction force of the swing leg are equal to zero); 2) the closed sagittal 7DOF model, which can be applied to model a double support

phase. These models can be applied to model kinematics and dynamics of normal gait in a sagittal plane over specific phases. An influence of the upper part of the body was modelled as the seventh segment, which gravity force acts at the center of mass placed at the point C_7 . Mathematical models of the open sagittal 7DOF model and closed sagittal 7DOF model are described in detail in [9]

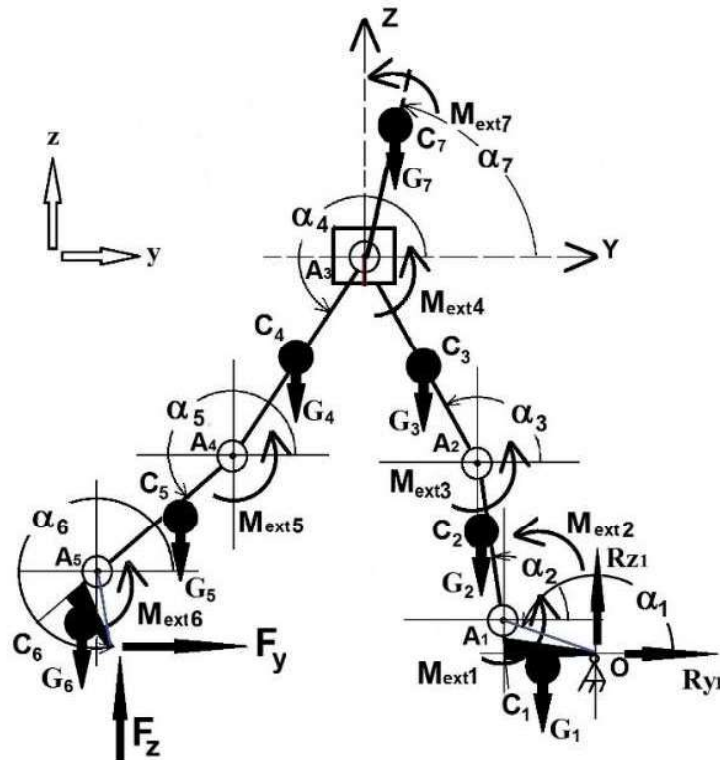


Figure 3. The sagittal 7DOF model (symbols are described in the Figure 2) [9]

Frontal 7DOF model

Considering a frontal plane and treating a body as a structure composed of seven segments serially linked through the hinge joints, there were created (Fig. 4): 1) the open frontal 7DOF model, which can be applied to model a single support phase (in this case both the x -th component of reaction force (R^F_{x2}) and the z -th component of reaction force (R^F_{z2}) are equal to zero); 2) the closed frontal 7DOF model, which can be used to describe a double support phase. Both models can be applied to analyze kinematics and dynamics of normal gait in a frontal plane during specific phases. An influence of the upper part of

the body was modelled as one concentrate force G_7 (it is a gravity force of upper part of the body) and its moment $M(b)$.

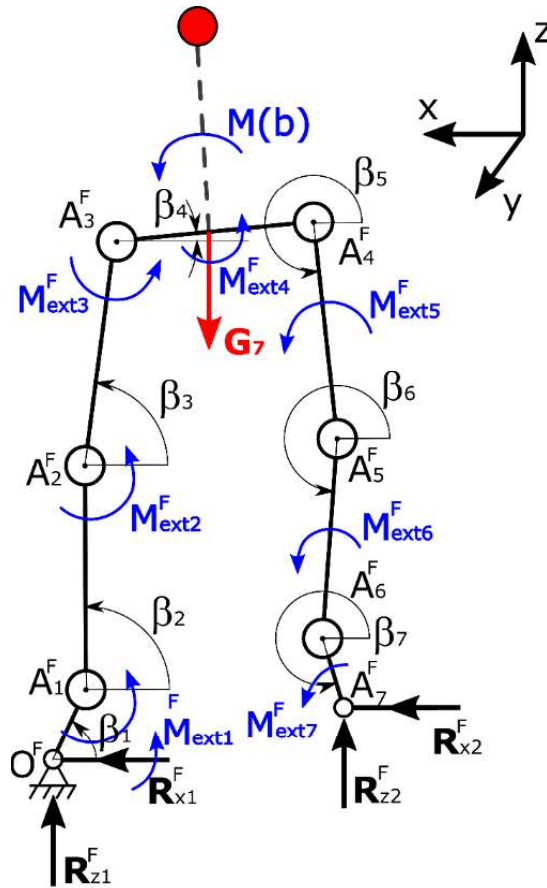


Figure 4. The frontal 7DOF model: (O^F – the point between the support foot and the ground; A^F_1 – the ankle joint of stance leg; A^F_2 – the knee joint of stance leg; A^F_3 – the stance leg hip joint; A^F_4 – the swing leg hip joint; A^F_5 – the knee joint of swing leg; A^F_6 – the ankle joint of swing leg; β_i – the angle of the i -th segment in the frontal plane (each angle is measured as an absolute coordinate); G – gravity force of the upper part of the body; M^F_{exti} – the external moment influenced the i -th segment in the frontal space; R^F_{x1} – the x -th component of stance leg reaction force (medio-lateral component); R^F_{z1} – the z -th component of the stance leg reaction force (vertical component); R^F_{x2} – the x -th component of reaction force during double support phase; R^F_{z2} – the z -th component of reaction force during double support phase; x – the transverse axis; y – the sagittal axis; z – the vertical axis)

A general mathematical description of the open frontal 7DOF model is a non-linear system of seven differential equations:

$$\begin{aligned}
 & B_{11} \cdot \ddot{\beta}_1 + B_{12}(\beta_1, \beta_2) \cdot \ddot{\beta}_2 + B_{13}(\beta_1, \beta_3) \cdot \ddot{\beta}_3 + B_{14}(\beta_1, \beta_4) \cdot \ddot{\beta}_4 + B_{15}(\beta_1, \beta_5) \cdot \ddot{\beta}_5 + \\
 & \quad + B_{16}(\beta_1, \beta_6) \cdot \ddot{\beta}_6 + B_{17}(\beta_1, \beta_7) \cdot \ddot{\beta}_7 = M_{1F} \\
 & B_{21}(\beta_1, \beta_2) \cdot \ddot{\beta}_1 + B_{22} \cdot \ddot{\beta}_2 + B_{23}(\beta_2, \beta_3) \cdot \ddot{\beta}_3 + B_{24}(\beta_2, \beta_4) \cdot \ddot{\beta}_4 + B_{25}(\beta_2, \beta_5) \cdot \ddot{\beta}_5 + \\
 & \quad + B_{26}(\beta_2, \beta_6) \cdot \ddot{\beta}_6 + B_{27}(\beta_2, \beta_7) \cdot \ddot{\beta}_7 = M_{2F} \\
 & B_{31}(\beta_1, \beta_3) \cdot \ddot{\beta}_1 + B_{32}(\beta_2, \beta_3) \cdot \ddot{\beta}_2 + B_{33} \cdot \ddot{\beta}_3 + B_{34}(\beta_3, \beta_4) \cdot \ddot{\beta}_4 + B_{35}(\beta_3, \beta_5) \cdot \ddot{\beta}_5 + \\
 & \quad + B_{36}(\beta_3, \beta_6) \cdot \ddot{\beta}_6 + B_{37}(\beta_3, \beta_7) \cdot \ddot{\beta}_7 = M_{3F} \\
 & B_{41}(\beta_1, \beta_4) \cdot \ddot{\beta}_1 + B_{42}(\beta_2, \beta_4) \cdot \ddot{\beta}_2 + B_{43}(\beta_3, \beta_4) \cdot \ddot{\beta}_3 + B_{44} \cdot \ddot{\beta}_4 + B_{45}(\beta_4, \beta_5) \cdot \ddot{\beta}_5 + \\
 & \quad + B_{46}(\beta_4, \beta_6) \cdot \ddot{\beta}_6 + B_{47}(\beta_4, \beta_7) \cdot \ddot{\beta}_7 = M_{4F} \\
 & B_{51}(\beta_1, \beta_5) \cdot \ddot{\beta}_1 + B_{52}(\beta_2, \beta_5) \cdot \ddot{\beta}_2 + B_{53}(\beta_3, \beta_5) \cdot \ddot{\beta}_3 + B_{54}(\beta_4, \beta_5) \cdot \ddot{\beta}_4 + B_{55} \cdot \ddot{\beta}_5 + \\
 & \quad + B_{56}(\beta_5, \beta_6) \cdot \ddot{\beta}_6 + B_{57}(\beta_5, \beta_7) \cdot \ddot{\beta}_7 = M_{5F} \\
 & B_{61}(\beta_1, \beta_6) \cdot \ddot{\beta}_1 + B_{62}(\beta_2, \beta_6) \cdot \ddot{\beta}_2 + B_{63}(\beta_3, \beta_6) \cdot \ddot{\beta}_3 + B_{64}(\beta_4, \beta_6) \cdot \ddot{\beta}_4 + \\
 & \quad + B_{65}(\beta_5, \beta_6) \cdot \ddot{\beta}_5 + B_{66} \cdot \ddot{\beta}_6 + B_{67}(\beta_6, \beta_7) \cdot \ddot{\beta}_7 = M_{6F} \\
 & B_{71}(\beta_1, \beta_7) \cdot \ddot{\beta}_1 + B_{72}(\beta_2, \beta_7) \cdot \ddot{\beta}_2 + B_{73}(\beta_3, \beta_7) \cdot \ddot{\beta}_3 + B_{74}(\beta_4, \beta_7) \cdot \ddot{\beta}_4 + \\
 & \quad + B_{75}(\beta_5, \beta_7) \cdot \ddot{\beta}_5 + B_{76}(\beta_6, \beta_7) \cdot \ddot{\beta}_6 + B_{77} \cdot \ddot{\beta}_7 = M_{7F}
 \end{aligned} \quad , \quad (1)$$

where β_i – the i -th angular displacement of the i -th segment (the i -th joint angle) in the frontal plane; $\dot{\beta}_i$ – the i -th angular velocity of the i -th segment in the frontal plane; $\ddot{\beta}_i$ – the i -th angular acceleration of the i -th segment in the frontal plane, $B_{ij}(\beta_i, \beta_j)$ – the ij -th coefficient depending on the mechanical characteristics.

A general mathematical description of the closed sagittal 7DOF model, which is an overactuated system, is a non-linear system of seven differential equations:

$$\begin{aligned}
 & B_{11} \cdot \ddot{\beta}_1 + B_{12}(\beta_1, \beta_2) \cdot \ddot{\beta}_2 + B_{13}(\beta_1, \beta_3) \cdot \ddot{\beta}_3 + B_{14}(\beta_1, \beta_4) \cdot \ddot{\beta}_4 + B_{15}(\beta_1, \beta_5) \cdot \ddot{\beta}_5 + \\
 & \quad + B_{16}(\beta_1, \beta_6) \cdot \ddot{\beta}_6 + B_{17}(\beta_1, \beta_7) \cdot \ddot{\beta}_7 = M_{1F} - L_1 \cdot \sin(\beta_1) \cdot R^F_{x2} + L_1 \cdot \cos(\beta_1) \cdot R^F_{z2} \\
 & B_{21}(\beta_1, \beta_2) \cdot \ddot{\beta}_1 + B_{22} \cdot \ddot{\beta}_2 + B_{23}(\beta_2, \beta_3) \cdot \ddot{\beta}_3 + B_{24}(\beta_2, \beta_4) \cdot \ddot{\beta}_4 + B_{25}(\beta_2, \beta_5) \cdot \ddot{\beta}_5 + \\
 & \quad + B_{26}(\beta_2, \beta_6) \cdot \ddot{\beta}_6 + B_{27}(\beta_2, \beta_7) \cdot \ddot{\beta}_7 = M_{2F} - L_2 \cdot \sin(\beta_2) \cdot R^F_{x2} + L_2 \cdot \cos(\beta_2) \cdot R^F_{z2} \\
 & B_{31}(\beta_1, \beta_3) \cdot \ddot{\beta}_1 + B_{32}(\beta_2, \beta_3) \cdot \ddot{\beta}_2 + B_{33} \cdot \ddot{\beta}_3 + B_{34}(\beta_3, \beta_4) \cdot \ddot{\beta}_4 + B_{35}(\beta_3, \beta_5) \cdot \ddot{\beta}_5 + \\
 & \quad + B_{36}(\beta_3, \beta_6) \cdot \ddot{\beta}_6 + B_{37}(\beta_3, \beta_7) \cdot \ddot{\beta}_7 = M_{3F} - L_3 \cdot \sin(\beta_3) \cdot R^F_{x2} + L_3 \cdot \cos(\beta_3) \cdot R^F_{z2} \\
 & B_{41}(\beta_1, \beta_4) \cdot \ddot{\beta}_1 + B_{42}(\beta_2, \beta_4) \cdot \ddot{\beta}_2 + B_{43}(\beta_3, \beta_4) \cdot \ddot{\beta}_3 + B_{44} \cdot \ddot{\beta}_4 + B_{45}(\beta_4, \beta_5) \cdot \ddot{\beta}_5 + \\
 & \quad + B_{46}(\beta_4, \beta_6) \cdot \ddot{\beta}_6 + B_{47}(\beta_4, \beta_7) \cdot \ddot{\beta}_7 = M_{4F} - L_4 \cdot \sin(\beta_4) \cdot R^F_{x2} + L_4 \cdot \cos(\beta_4) \cdot R^F_{z2} \\
 & B_{51}(\beta_1, \beta_5) \cdot \ddot{\beta}_1 + B_{52}(\beta_2, \beta_5) \cdot \ddot{\beta}_2 + B_{53}(\beta_3, \beta_5) \cdot \ddot{\beta}_3 + B_{54}(\beta_4, \beta_5) \cdot \ddot{\beta}_4 + B_{55} \cdot \ddot{\beta}_5 + \\
 & \quad + B_{56}(\beta_5, \beta_6) \cdot \ddot{\beta}_6 + B_{57}(\beta_5, \beta_7) \cdot \ddot{\beta}_7 = M_{5F} - L_5 \cdot \sin(\beta_5) \cdot R^F_{x2} + L_5 \cdot \cos(\beta_5) \cdot R^F_{z2} \\
 & B_{61}(\beta_1, \beta_6) \cdot \ddot{\beta}_1 + B_{62}(\beta_2, \beta_6) \cdot \ddot{\beta}_2 + B_{63}(\beta_3, \beta_6) \cdot \ddot{\beta}_3 + B_{64}(\beta_4, \beta_6) \cdot \ddot{\beta}_4 + \\
 & \quad + B_{65}(\beta_5, \beta_6) \cdot \ddot{\beta}_5 + B_{66} \cdot \ddot{\beta}_6 + B_{67}(\beta_6, \beta_7) \cdot \ddot{\beta}_7 = M_{6F} - L_6 \cdot \sin(\beta_6) \cdot R^F_{x2} + L_6 \cdot \cos(\beta_6) \cdot R^F_{z2} \\
 & B_{71}(\beta_1, \beta_7) \cdot \ddot{\beta}_1 + B_{72}(\beta_2, \beta_7) \cdot \ddot{\beta}_2 + B_{73}(\beta_3, \beta_7) \cdot \ddot{\beta}_3 + B_{74}(\beta_4, \beta_7) \cdot \ddot{\beta}_4 + \\
 & \quad + B_{75}(\beta_5, \beta_7) \cdot \ddot{\beta}_5 + B_{76}(\beta_6, \beta_7) \cdot \ddot{\beta}_6 + B_{77} \cdot \ddot{\beta}_7 = M_{7F} - M(R^F_{x2}) + M(R^F_{z2})
 \end{aligned} \quad , \quad (2)$$

where $M(R^F_{x2})$ and $M(R^F_{z2})$ – moments originating from the components of interaction reaction that influence the seventh segment $A^F_6A^F_7$ (Fig. 4); L_i – length of the i -th segment that is placed under the i -th angle β_i .

Approaches for interaction modelling

In order to study an influence of interaction one could apply two approaches: the first one for inverse dynamic problem solution; the second one for forward dynamic task solution. According to the first approach, measured ground force values (the y -th component (F_y) and z -th component (F_z) in each sagittal model; the x -th component (R^F_{x2}) and z -th component (R^F_{z2}) in the frontal model) influenced by an interaction with the ground can be inputted into the chosen model. These values can be measured by using a second force plate. According to the second approach, an interaction with a ground can be modelled by applying an additional analytical model that estimates the value of external load needed to stay a strike foot in the narrow range of the ground level [9].

3. Results

A validation of proposed biomechanical models had been performed by solving an inverse dynamic task without using any optimization approach. To compare measured data with calculated ones the experimental researches had conducted on the group of health males. In this paper there are presented results of validation for one random chosen male person (body mass 72.2 kg and body height 177.5 cm) (Fig.5A). To obtain kinematic data there was used a marker setting (Rizzoli protocol) of OPTITRACK system composed of six cameras working with 120 Hz frequency and dedicated software (Fig.5B-5C). To measure kinetic data (interaction forces) the Steinbichler force plate was applied. A subject was given an oral instruction. This subject did five successful trials (each trial contained three full steps) by walking barefoot in preferred speed with open eyes. Specific gait phases were defined on the base of the analysis of the posture reproduced by the motion capture system (Fig. 6).

Applying Zatsiorsky's segmentation method and principles of mechanics, centers of gravity of all segments (right and left foot, right and left calf, right and left thigh, upper body part) were calculated for each frame recorded by the motion capture system. It was also assumed that the subject examined was in a homogenous gravity field (gravity acceleration equals to $g = 9.8 \text{ m/s}^2$).

On the base of markers' displacements there were calculated angular displacements of all segments of the body: a) in a sagittal plane (in Fig. 7 relative angular displacements are given as $Hip = \alpha_3 - \alpha_7$, $Knee = \alpha_3 - \alpha_2$ and $Ankle = \alpha_1 - \alpha_2 - \pi/2$ [7]); b) in a frontal plane (Fig. 8). To estimate segment angular velocities and segment angular acceleration, the kinematic data were processed by applying: 1) filtering (the Butterworth filter of the fourth order with 5Hz cut-off frequency was applied); 2) cubic spline interpolation; 3) differentiation by applying three-point difference method.

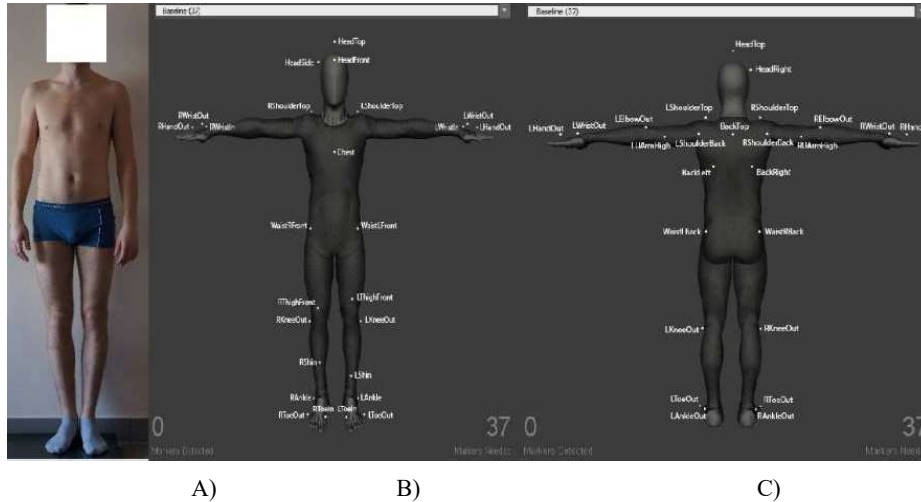


Figure 5. A) a subject examined; B) marker setting (anterior); C) marker setting (posterior)

A validation was performed by comparing a vertical component of interaction measured during single phase with a vertical component of interaction calculated by applying a sagittal 6DOF model (Fig. 9), sagittal 7DOF model (Fig. 10) and frontal 7DOF model (Fig. 11). Moreover, there were also compared data referring to a horizontal component of interaction measured during this phase and a horizontal component of interaction calculated by applying a sagittal 6DOF model (Fig. 12), sagittal 7DOF model (Fig. 13) and frontal 7DOF model (Fig. 14). Due to the fact that only one force plate was available in practice, we limited a validation of our models only to the single phase of the gait.

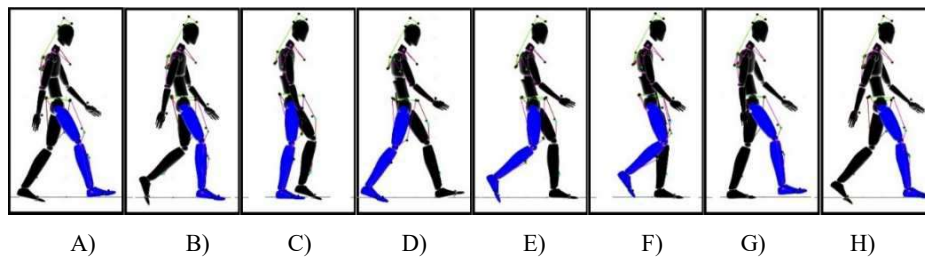


Figure 6. Posture setting during the one full step of the gait: A) Double support phase; B) Single support phase (foot-flat of right leg and toe-off of left leg); C) Single support phase (stance of right leg and deceleration of swing left leg); D) Double support phase; E) Single support phase (foot-flat of left leg and toe-off of right leg); F) Single support phase (stance of left leg and swing right leg); G) Single support phase (stance of left leg and deceleration of swing right leg); H) Double support phase [8-9]

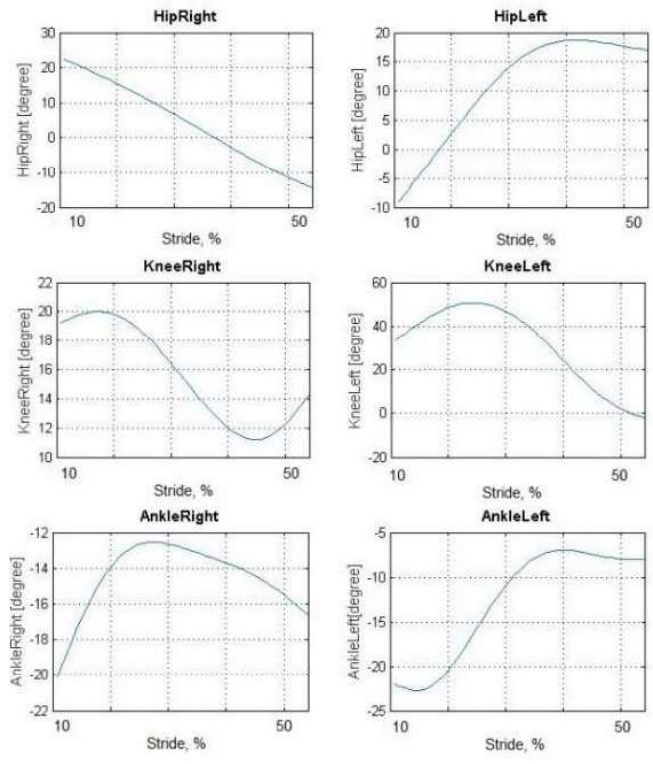


Figure 7. Kinematic data (sagittal plane)

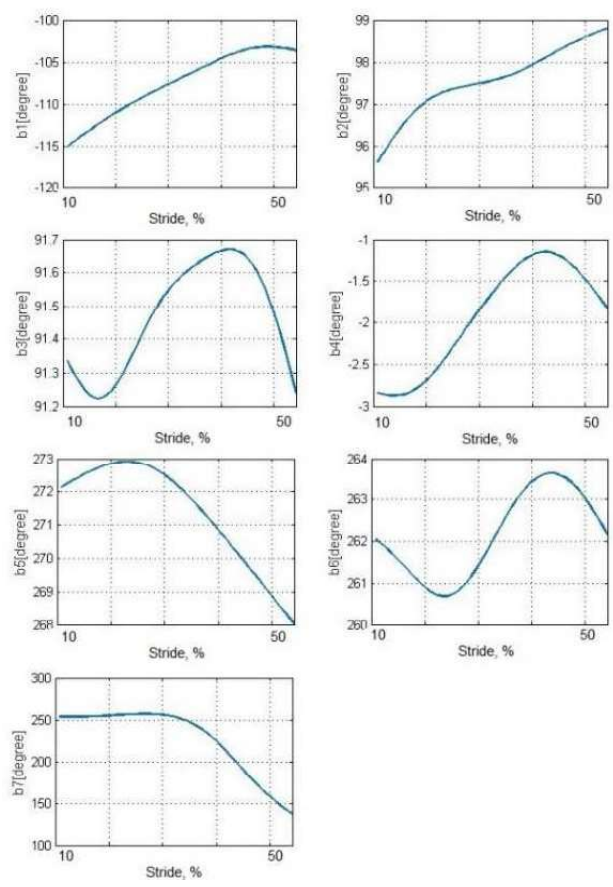


Figure 8. Kinematic data (frontal plane)

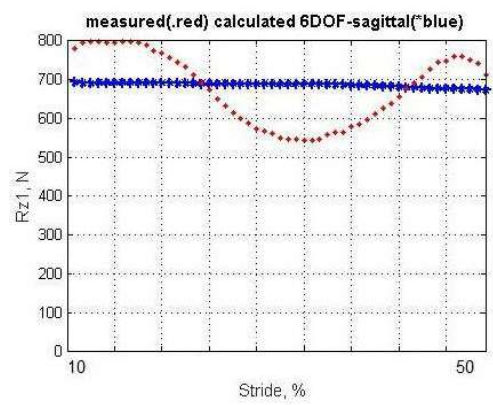


Figure 9. Vertical component of interaction: measured component and calculated component for sagittal 6DOF model

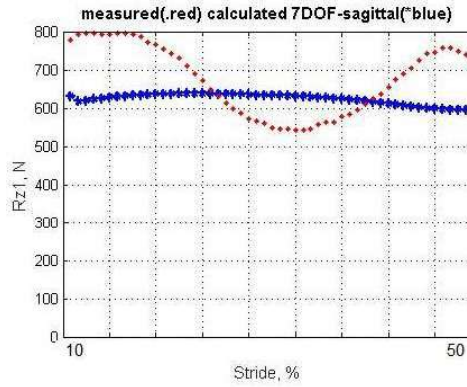


Figure 10. Vertical component of interaction: measured component and calculated component for sagittal 7DOF model

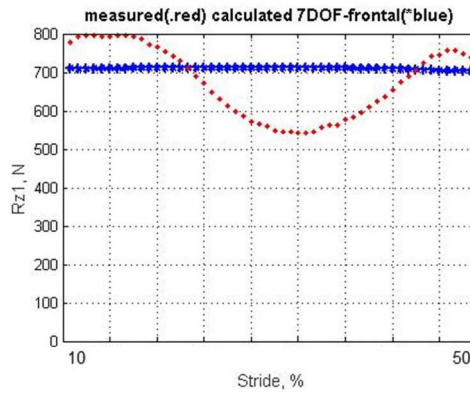


Figure 11. Vertical component of interaction: measured component and calculated component for frontal 7DOF model

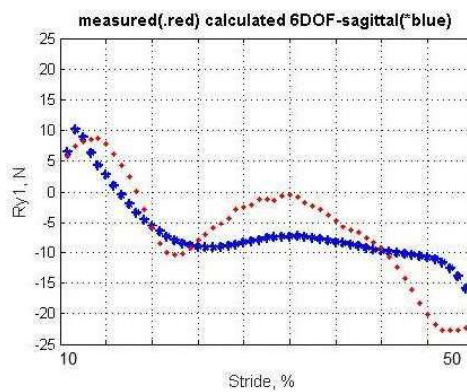


Figure 12. Horizontal component of interaction: measured component (towards sagittal axis) and calculated component for sagittal 6DOF model

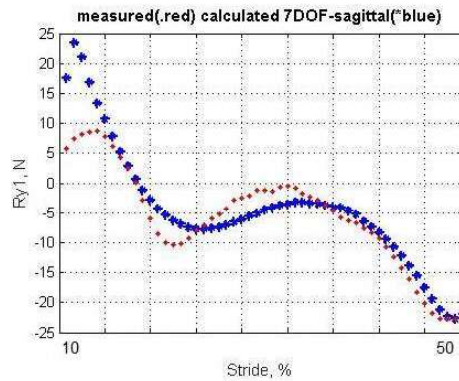


Figure 13. Horizontal component of interaction: measured component (towards sagittal axis) and calculated component for sagittal 7DOF model

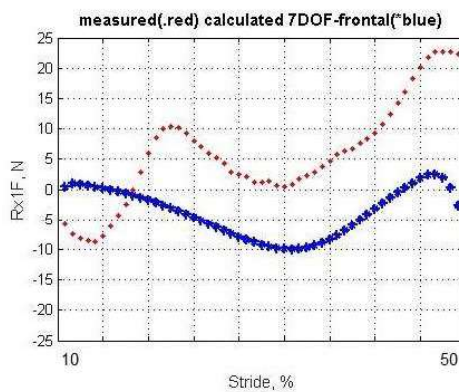


Figure 14. Horizontal component of interaction: measured component (towards transverse axis) and calculated component for frontal 7DOF model

4. Discussion

On the base of the obtained data (measured and calculated) given in the section 3, we concluded that over single support phase:

- all three vertical components of interaction calculated by using a sagittal 6DOF model (Fig. 9), sagittal 7DOF model (Fig. 10) and frontal 7DOF model (Fig. 11) have very similar shapes and values that are approximate to the measured one. Values of absolute relative error of calculated component with respect to the measured one are following: 26.7% (sagittal 6DOF model (Fig. 9)), 22.2% (sagittal 7DOF model (Fig. 10)) and 31.4% (frontal 7DOF model (Fig. 11));
- the horizontal component calculated by the sagittal 6DOF model (Fig. 12) and sagittal 7DOF model (Fig. 13) is closely approximated to the measured horizontal one;

- the horizontal component calculated by the frontal 7DOF model (Fig. 14) has only slightly similar shape with respect to the measured horizontal one. This discrepancy is observed in the small range of force value.

It is worth emphasizing that calculated components were obtained without applying any optimization approach that could be used to fit the calculated data with the calculated ones. Considering presented results of validation, one should keep in mind that following factors are very crucial and have a big impact on the calculated results:

- 1) a method of segmentation used to calculate segment masses, segment lengths, segment radii of gyration (in the study it was applied Zatsiorsky's method, which assumes that each segment is a homogenous cylinder);
- 2) segment moments of inertia that influence dynamics of system considered (in this study a Zatsiorsky's method was used to calculate segment moments of inertia);
- 3) methods applied for kinematic data processing that are used to calculate segment angular velocities and segment angular accelerations (data processing should constrain non-physiological jerks);
- 4) data that describe the upper body part influence in each planar model (location of mass of upper body with respect to the hip joints of each model);
- 5) data that describe the seventh segment of the sagittal 7DOF model (mass m_7 , length L_7 , radius of gyration S_7 and moment of inertia J_7).

5. Conclusions

The aim of this study was to create multibody biomechanical models that can be used to analyze a normal gait of the human and to identify joint moments of the lower limbs during normal gait in the single and the double support phase. Applying Newton-Euler formulation, six planar biomechanical models were developed: 1) a mathematical 6DOF model describing gait in the sagittal plane of the body for single support phase (open sagittal 6DOF model); 2) a mathematical 6DOF model describing a gait in the sagittal plane of the body for double support phase (closed sagittal 6DOF model); 3) a mathematical 7DOF model describing a gait in the sagittal plane of the body for single support phase (open sagittal 7DOF model); 4) a mathematical 7DOF model describing a gait in the sagittal plane of the body for double support phase (closed sagittal 7DOF model); 5) a mathematical 7DOF model describing a gait in the frontal plane of the body for single support phase (open frontal 7DOF model); 6) a mathematical 7DOF model describing a gait in the frontal plane of the body for double support phase (closed frontal 7DOF model). Proposed mathematical models can be applied to solve a forward dynamic task or an inverse dynamic task. A validation of these models had been performed by comparing results measured over examination of normal human gait with calculated ones obtained by

solving an inverse dynamic task. Applying a sagittal 7DOF model, the influence of the moment of inertia of the upper body is taken into account, whereas the sagittal 6DOF model and the frontal 7DOF model only consider an influence of upper body load. Due to the fact that proposed biomechanical models only describe planar motions, they should be applied with caution to analyze an asymmetrical gait.

Applying models presented in this paper, one can assess joint moments and joint intersegmental forces that origin due to influence of elements linking neighboring segments. These elements model an influence of soft tissues that are bending each joint (ligaments, bursa, muscles with tendons) and also affecting acceleration or deceleration of segments, especially at the end of the range of motion. Moreover, joint moments and joint intersegmental forces are produced due to interaction (contact) between the components of musculoskeletal system. On the base of calculated kinematic and kinetic data one can assess power produced by the chosen segments and joint powers produced by the chosen joints of the lower limb. However, one should take in mind that application of an inverse dynamic approach does not allow to consider influence of multi-joint muscles and to detect a co-contraction phenomenon that is very important to maintain a stable posture [9]. Proposed biomechanical models can be used to obtain data to design a mechanical construction of the exoskeleton used to enhance performance of the lower limbs. Also, these models can be used to design a control system of this exoskeleton to enhance the given motion performance by keeping the chosen range of the human locomotive stability. Moreover, considering motions of the human, one should keep in mind that all motions are performed in some range of variability [10].

It is worth remembering that planar models presented in this paper cannot model phenomena occurring due to rotations in the transverse plane, since presented models only describe phenomena occurring towards a medio-lateral axis of rotation (in the sagittal plane of the body) and anterior-posterior axis of rotation (in the frontal plane of the body).

Acknowledgments

The work has been supported by the Polish National Science Centre under the grant OPUS 9 No. 2015/17/B/ST8/01700 for years 2016-2018. Calculations were carried out at the Academic Computer Centre in Gdansk, Poland.

References

- [1] Awrejcewicz J.: Classical Mechanics. Dynamics. Springer Berlin (2012).
- [2] De Leva P. Adjustments to Zatsiorsky-Seluyanov's segment inertia parameters. *Journal of Biomechanics* 29 (9), 1996, 1223–1230 (1996)



- [3] De Leva P.: Joint center longitudinal positions computed from a selected subset of Chandlers' data. *J Biomech* 29 (9), 1231–1233 (1996)
- [4] Grzelczyk D., Awrejcewicz J.: Modeling and control of an eight-legged walking robot driven by different gait generators. *International Journal of Structural Stability and Dynamics* (in press). doi: 10.1142/S0219455419410098
- [5] Onyshko S., Winter D.A.: A mathematical model for the dynamics of human locomotion. *J Biomechanics* 13, 361-368 (1980)
- [6] Troy J.J.: Dynamic balance and walking control of biped mechanisms. *Retrospective Theses and Dissertations*, 11095, Iowa State University (1995)
- [7] Winter D.A.: Overall principle of lower limb support during stance phase of gait. *J Biomech* 13, 923–927 (1980)
- [8] Wojnicz W., Zagrodny B., Ludwicki M., Syczewska M., J. Mrozowski, Awrejcewicz J.: Approach for determination of functioning of lower limb muscles. *Dynamical Systems in Applications* (ed. J. Awrejcewicz). *Springer Proceedings in Mathematics & Statistics*, Vol. 249, 423–38 (2018)
- [9] Wojnicz W.: *Biomechaniczne modele układu mięśniowo-szkieletowego człowieka* (Biomechanical models of the human musculoskeletal system). Wydawnictwo Politechniki Gdańskiej, Gdańsk, Poland, 1-209, ISBN 978-83-7348-727-7 (2018)
- [10] Zagrodny B., Ludwicki M., Wojnicz W., Mrozowski J., Awrejcewicz J.: Cooperation of mono- and bi-articular muscles: human lower limb. *Journal of Musculoskeletal and Neuronal Interactions*, 1–7 (2018)
- [11] Zajac F.E., Neptune R.R., Kautz S.A.: Biomechanics and muscle coordination of human walking. Part I: Introduction to concepts, power transfer, dynamics and simulations. *Gait Posture* 16, 215–232 (2002)
- [12] Yamaguchi G.T., Zajac F.E.: Restoring Unassisted natural gait to paraplegics via functional neuromuscular stimulation: a computer simulation study. *IEEE Transactions on biomedical engineering* 37 (9), 886-902 (1990)

Wiktoria Wojnicz, Ph.D. DSc, Associate Professor: Gdansk University of Technology, str. G. Narutowicza 11/12, 80-233 Gdansk, POLAND (wiktoria.wojnicz@pg.edu.pl). The author gave a presentation of this paper during one of the conference sessions.

Bartłomiej Zagrodny, Ph.D.: Lodz University of Technology, str. Stefanowskiego 1/15, 90-924 Lodz, POLAND (bartlomiej.zagrodny@p.lodz.pl).

Michał Ludwicki, Ph.D.: Lodz University of Technology, str. Stefanowskiego 1/15, 90-924 Lodz POLAND (michal.ludwicki@p.lodz.pl).

Jerzy Mrozowski, Ph.D., DSc, Associate Professor: Lodz University of Technology, str. Stefanowskiego 1/15, 90-924 Lodz POLAND (jerzy.mrozowski@p.lodz.pl).

Jan Awrejcewicz, Professor: Lodz University of Technology, str. Stefanowskiego 1/15, 90-924 Lodz, POLAND (jan.awrejcewicz@p.lodz.pl).

Edmund Wittbrodt, Professor.: Gdansk University of Technology, str. G. Narutowicza 11/12, 80-233 Gdansk, POLAND (Edmund.wittbrodt@pg.edu.pl).

